

UCRL-JRNL-221555



LAWRENCE  
LIVERMORE  
NATIONAL  
LABORATORY

# Determining (n,f) cross sections for actinide nuclei indirectly: An examination of the Surrogate Ratio Method

J. E. Escher, F. S. Dietrich

May 23, 2006

Physical Review C

## **Disclaimer**

---

This document was prepared as an account of work sponsored by an agency of the United States Government. Neither the United States Government nor the University of California nor any of their employees, makes any warranty, express or implied, or assumes any legal liability or responsibility for the accuracy, completeness, or usefulness of any information, apparatus, product, or process disclosed, or represents that its use would not infringe privately owned rights. Reference herein to any specific commercial product, process, or service by trade name, trademark, manufacturer, or otherwise, does not necessarily constitute or imply its endorsement, recommendation, or favoring by the United States Government or the University of California. The views and opinions of authors expressed herein do not necessarily state or reflect those of the United States Government or the University of California, and shall not be used for advertising or product endorsement purposes.

# Determining (n,f) cross sections for actinide nuclei indirectly: An examination of the Surrogate Ratio Method

Jutta E. Escher\* and Frank S. Dietrich†

*Lawrence Livermore National Laboratory, Livermore, CA 94550*

(Dated: May 22, 2006)

The validity of the Surrogate Ratio method for determining (n,f) cross sections for actinide nuclei is examined. This method relates the ratio of two compound-nucleus reaction cross sections to a ratio of coincidence events from two measurements in which the same compound nuclei are formed via a direct reaction. With certain assumptions, the method allows one of the cross sections to be inferred if the other is known. We develop a nuclear reaction-model simulation to investigate whether the assumptions underlying the Ratio approach are valid and employ these simulations to assess whether the cross sections obtained indirectly by applying a Ratio analysis agree with the expected results. In particular, we simulate Surrogate experiments that allow us to determine fission cross sections for selected actinide nuclei. The nuclei studied,  $^{233}\text{U}$  and  $^{235}\text{U}$ , are very similar to those considered in recent Surrogate experiments. We find that in favorable cases the Ratio method provides useful estimates of the desired cross sections, and we discuss some of the limitations of the approach.

PACS numbers: 25.85.Ec, 24.60.Dr, 24.50.+g, 27.90.+b

## I. INTRODUCTION

Nuclear reaction data play an important role in nuclear physics applications. Unfortunately, for a large number of reactions the relevant data cannot be directly measured in the laboratory or reliably predicted by calculations. Direct measurements of reactions on unstable isotopes are particularly affected since the relevant nuclei are often too difficult to produce with currently available experimental techniques or too short-lived to serve as targets in present-day set-ups. Calculations are highly nontrivial since they typically require a thorough understanding of both direct and statistical reaction mechanisms (as well as their interplay) and a detailed knowledge of the nuclear structure involved. It is therefore important to explore alternative approaches for determining reaction cross sections on unstable nuclei.

The “Surrogate Reaction Method” is a specific indirect method that combines experiment with reaction theory to obtain cross sections for compound-nucleus reactions involving difficult-to-produce targets. While the Surrogate method is very general and can in principle be employed to determine cross sections for all types of compound-nucleus reactions involving a large variety of target nuclei, there are various challenges that have to be addressed in order to validate and implement this approach for the different regions of interest in the nuclear chart. For applications to (n,f) cross sections on actinide nuclei, Younes and Britt have studied some of these issues recently [1, 2]. For applications to (n, $\gamma$ ) cross sections on lighter nuclei, in particular on s-process branch points, work is currently underway [3–7].

It is useful to consider whether certain simplifications or approximations to the method can be utilized to determine relevant cross sections. A simple, approximate version of the Surrogate technique, which we will refer to as the “Surrogate Method in the Weisskopf-Ewing limit” was already used in the 1970s to estimate neutron-induced fission cross sections from transfer reactions [8–12] and has received renewed attention in recent years [13]. In the work presented here, we will focus on a related approximation, the so-called “Surrogate Ratio Method” or simply the “Ratio Method”.

The purpose of this paper is an examination of the validity of the Surrogate Ratio method for determining (n,f) cross sections for actinide nuclei. The study was motivated by recent (d,d’f) and ( $\alpha,\alpha'$ f) Surrogate experiments at Yale [14] and Berkeley [15], respectively, which were analyzed in the framework of the Ratio approach. In the present study we will use a nuclear reaction-model simulation to investigate whether the assumptions underlying the Ratio method are valid, and employ these simulations to assess whether the cross section obtained indirectly by applying the Ratio method agrees with the expected result. We will also comment on the validity of the Surrogate Method in the Weisskopf-Ewing limit, since it is closely related to the Ratio approach.

The experiments described in [14, 15] investigated indirectly neutron-induced fission for  $^{235}\text{U}$  and  $^{237}\text{U}$ , while we chose to focus on (n,f) reactions on  $^{233}\text{U}$  and  $^{235}\text{U}$ . This choice has the advantage that we study nuclei which are very similar to those considered in the recent experiments, but for which all of the relevant cross sections are known from direct measurements. Therefore, the results of the present study can be used to reach conclusions about the accuracy of the Ratio technique for measuring the previously unknown  $^{237}\text{U}$ (n,f) cross section.

This document is organized as follows: In the next section, we will introduce the main concepts employed

---

\*Electronic address: [escher1@llnl.gov](mailto:escher1@llnl.gov)

†Electronic address: [dietrich2@llnl.gov](mailto:dietrich2@llnl.gov)

in the present report. In particular, we will explain the Surrogate method, review the Weisskopf-Ewing approximation to the method, and introduce the Ratio approach. In Section III we describe the simulations we are using and outline the logic of the tests we are carrying out in order to assess the validity of the Ratio method. In Section IV we present calculations that test the primary assumption underlying the Ratio approach, the validity of the Weisskopf-Ewing approximation. We then compare cross section predictions of both the Surrogate Method in the Weisskopf-Ewing limit and the Surrogate Ratio method to predetermined reference cross sections. Our findings and conclusions are summarized in Section V.

## II. SURROGATE APPROACHES

This section introduces the main concepts employed in this study. The Surrogate idea is explained and the challenges associated with carrying out, analyzing, and interpreting a Surrogate experiment are outlined. The

Weisskopf-Ewing limit of the full Hauser-Feshbach theory is briefly reviewed in the context of Surrogate reactions and the Ratio Method, which makes use of the Surrogate idea and assumes the validity of the Weisskopf-Ewing approximation, is introduced.

### A. The Surrogate Idea

The Surrogate nuclear reaction technique is an indirect method for determining the cross section for a particular type of “desired” reaction, namely a two-step reaction,  $a + A \rightarrow B^* \rightarrow c + C$ , that proceeds through a compound nuclear state  $B^*$ , a highly excited state in statistical equilibrium (see Figure 1).

The formalism appropriate for describing compound-nucleus reactions is the statistical Hauser-Feshbach theory (see, *e.g.*, chapter 10 of Ref. [16]). The average cross section per unit energy in the outgoing channel  $\chi'$  for reactions proceeding to an energy region in the final nucleus described by a level density is given by:

$$\frac{d\sigma_{\alpha\chi}^{HF}(E_\alpha)}{dE_{\chi'}} = \pi\lambda_\alpha^2 \sum_{J\pi} \omega_\alpha^J \sum_{ls'l's'I'} \frac{T_{\alpha ls}^J(E_\alpha) T_{\chi'l's'}^J(E_{\chi'}) \rho_{I'}(U')}{\sum_{\chi''l''s''I''} T_{\chi''l''s''}^J(E_{\chi''}) + \sum_{\chi''l''s''I''} \int T_{\chi''l''s''}^J(E_{\chi''}) \rho_{I''}(U'') dE_{\chi''}}. \quad (1)$$

Here  $\alpha$  denotes the entrance channel  $a + A$  with energy  $E_\alpha$  and reduced wavelength  $\lambda_\alpha$ . The spin of the incident particle is  $i$ , the target spin is  $I$ , the channel spin is  $\vec{s} = \vec{i} + \vec{I}$ , and the compound-nucleus angular momentum and parity are  $J, \pi$ . The excitation energy of the compound nucleus,  $E_{ex}$ , is related to  $E_\alpha$  via the separation energy  $S_a(B)$  of the particle  $a$  in the nucleus  $B$ :  $E_{ex} = S_a(B) + E_\alpha$ . The transmission coefficient associated with the entrance channel is denoted  $T_{\alpha ls}^J$  and the statistical-weight factor  $\omega_\alpha^J$  is given by  $(2J+1)/[(2i+1)(2I+1)]$ . Quantities associated with the exit channel of interest are denoted by primed symbols:  $\chi' = c' + C'$ ,  $i'$  is the spin of the outgoing particle  $c'$ ,  $I'$  is the spin of the residual nucleus  $C'$ ,  $\vec{s}' = \vec{i}' + \vec{I}'$  is the channel spin and  $E_{\chi'}$  the energy for  $\chi'$ . The energy of the decaying nucleus,  $E_{ex}$ , is related to  $E_{\chi'}$  via the relation  $E_{ex} = S_{c'}(B) + E_{\chi'}$ , where  $S_{c'}(B)$  is the separation energy of  $c'$  in  $B$ . The transmission coefficients for this channel are written as  $T_{\chi'l's'}^J(E_{\chi'})$  and  $\rho_{I'}(U')$  denotes the density of levels of spin  $I'$  at excitation energy  $U'$  in the residual nucleus  $C'$ . All energetically possible final channels  $\chi''$  have to be taken into account, thus the denominator includes contributions from decays to discrete levels in the residual nuclei (given by the sum  $\sum'$ ) as well as contributions from decays to regions of high level density in the residual nuclei (given by the second sum in the denominator which involves an energy

integral of transmission coefficients and level densities in the residual nuclei). The relevant quantities in these final channels  $\chi''$  are denoted by double-primed symbols, in analogy to the particular channel of interest,  $\chi'$ . In writing Eq. 1, we have suppressed the parity quantum number except for that of the compound nucleus. The level density depends in principle on parity (even though this dependence is weak in practice), and all sums over quantum numbers must respect angular-momentum and parity conservation.

The above Hauser-Feshbach formula neglects correlations between the incident and outgoing reaction channels that can be taken into account formally by including width fluctuation corrections. These correlations enhance the elastic scattering cross section and reduce the inelastic and reaction cross sections, although this depletion rarely exceeds 10-20% (even at energies below approximately 2 MeV) and becomes negligible as the excitation energy of the compound nucleus increases. In the remainder of this study we will neglect width fluctuation corrections and rewrite the Hauser-Feshbach formula as:

$$\frac{d\sigma_{\alpha\chi}^{HF}(E_\alpha)}{dE_\chi} = \sum_{J\pi} \sigma_\alpha^{CN}(E_{ex}, J, \pi) G_\chi^{CN}(E_{ex}, J, \pi), \quad (2)$$

where  $\sigma_\alpha^{CN}(E_{ex}, J, \pi)$  denotes the cross section for forming the compound nucleus at excitation energy  $E_{ex}$  with angular-momentum and parity quantum numbers  $J\pi$  in

the reaction  $a + A \rightarrow B^*$ . The symbol  $G_\chi^{CN}(E_{ex}, J, \pi)$  is the branching ratio for the decay of this compound state into the desired exit channel  $\chi$ . Here and in the remainder of the paper we suppress the prime associated with the exit channel of interest, unless it is necessary to distinguish explicitly between all possible final channels ( $\chi''$ ) and the particular channel of interest ( $\chi'$ ).

In the limit of negligible width fluctuation corrections considered here, the formation and decay of the compound nucleus are independent of each other, individually for each angular momentum and parity value. It is this independence that allows one to determine the desired cross section via a combination of theory and experiment in the Surrogate approach. In many cases the formation cross section  $\sigma_\alpha^{CN}$  can be calculated to a reasonable accuracy by using optical potentials while the theoretical branching ratios  $G_\chi^{CN}$  for the different channels  $\chi$  are often quite uncertain. The objective of the Surrogate method is to determine or constrain these decay probabilities experimentally.

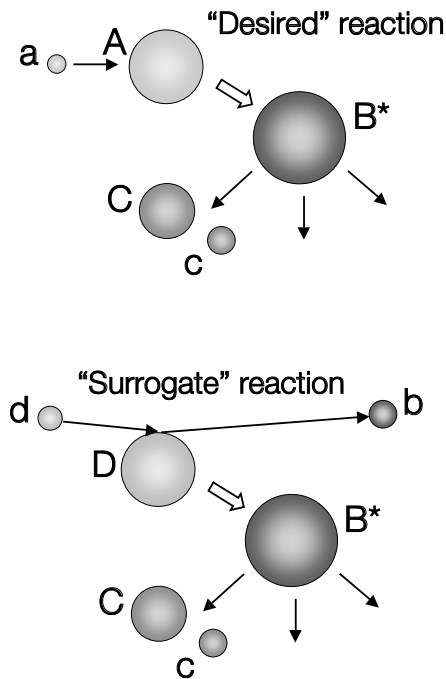


FIG. 1: Schematic representation of the “desired” (top) and “Surrogate” (bottom) reaction mechanisms. The basic idea of the Surrogate approach is to replace the first step of the desired reaction,  $a + A$ , by an alternative (“Surrogate”) reaction,  $d + D \rightarrow b + B^*$ , that populates the same compound nucleus. The subsequent decay of the compound nucleus into the relevant channel can then be measured and used to extract the desired cross section.

In a Surrogate experiment, the compound nucleus  $B^*$  is produced via an alternative (“Surrogate”), direct reaction  $d + D \rightarrow b + B^*$  and the decay of  $B^*$  is observed

in coincidence with the outgoing particle  $b$ . The direct-reaction particle is typically stopped in a detector which provides particle identification, as well as information on the kinetic energy and direction of  $b$ . The desired exit channel  $\chi$  can be identified, *e.g.*, by detecting fission fragments from  $B^*$  or  $\gamma$  rays from the desired residual nucleus  $C$ . The probability for forming  $B^*$  in the Surrogate reaction (with specific values for  $E_{ex}$ ,  $J$ ,  $\pi$ ) is  $F_\delta^{CN}(E_{ex}, J, \pi)$ , where  $\delta$  refers to the reaction  $d + D \rightarrow b + B^*$ . The quantity

$$P_{\delta\chi}(E_{ex}) = \sum_{J,\pi} F_\delta^{CN}(E_{ex}, J, \pi) G_\chi^{CN}(E_{ex}, J, \pi), \quad (3)$$

which gives the probability that the compound nucleus  $B^*$  was formed with energy  $E_{ex}$  and decayed into channel  $\chi$ , can be obtained experimentally. The direct-reaction probabilities  $F_\delta^{CN}(E_{ex}, J, \pi)$ , where  $\sum_{J,\pi} F_\delta^{CN}(E_{ex}, J, \pi) = 1$ , have to be determined theoretically. In practice, the decay of the compound nucleus is modeled and the  $G_\chi^{CN}(E_{ex}, J, \pi)$  are obtained by adjusting parameters in the model to reproduce the measured decay probabilities  $P_{\delta\chi}(E_{ex})$ . Subsequently, the branching ratios obtained in this manner are inserted in Eq. 2 to yield the desired reaction cross section. In the above discussion, we have omitted the angular dependence of both the desired and the Surrogate reactions on the observation angle of the particles emitted from the compound nucleus  $B^*$ . The extension of the Hauser-Feshbach formulae is straightforward [16].

In practice the procedure of determining the branching ratios is a difficult task due to several theoretical and experimental challenges: i) The decay probability  $P_{\delta\chi}(E_{ex}) = N_{\delta\chi}(E_{ex})/N_\delta(E_{ex})$  is experimentally determined: Here  $N_\delta$  denotes the total number of  $d + D \rightarrow b + B^*$  reactions, usually determined by observing the outgoing particle  $b$ , and  $N_{\delta\chi}$  is the number of  $b$ - $\chi$  coincidences. Both  $N_{\delta\chi}$  and  $N_\delta$  need to be accurately determined. If target contaminants are present, it becomes very difficult, if not impossible to determine a reliable value for  $N_\delta$ . ii) The theoretical prediction of the direct-reaction probabilities  $F_\delta^{CN}(E_{ex}, J, \pi)$  requires a framework for calculating cross sections of direct reactions (stripping, pick-up, and inelastic scattering) to continuum states in  $B^*$ . iii) Extracting the branching ratios  $G_\chi^{CN}(E_{ex}, J, \pi)$  from measured decay probabilities  $P_{\delta\chi}(E_{ex})$  requires modeling the decay of the compound nucleus produced in the Surrogate reaction and fitting the relevant parameters to reproduce the experimental results. iv) The possibility that the intermediate nucleus  $B^*$  produced in the Surrogate reaction decays before statistical equilibrium is reached has to be excluded or minimized.

## B. The Weisskopf-Ewing Limit

The Hauser-Feshbach theory rigorously conserves total angular momentum  $J$  and parity  $\pi$ . Under certain

conditions the branching ratios  $G_\chi^{CN}(E_{ex}, J, \pi)$  can be treated as independent of  $J$  and  $\pi$  and the form of the cross section (for the desired reaction) simplifies to

$$\frac{d\sigma_{\alpha\chi}^{WE}(E_a)}{dE_\chi} = \sigma_\alpha^{CN}(E_{ex}) \mathcal{G}_\chi^{CN}(E_{ex}) \quad (4)$$

where

$$\begin{aligned} \sigma_\alpha^{CN}(E_{ex}) &= \sum_{J,\pi} \sigma_\alpha^{CN}(E_{ex}, J, \pi) \\ &= \pi\lambda_\alpha^2 \sum_{l=0}^{\infty} (2l+1) T_{\alpha l}(E_\alpha) \end{aligned} \quad (5)$$

is the reaction cross section describing the formation of the compound nucleus at energy  $E_{ex}$  and  $\mathcal{G}_\chi^{CN}(E_{ex})$  denotes the  $J\pi$ -independent branching ratio for the exit channel  $\chi$ . This is the Weisskopf-Ewing limit of the Hauser-Feshbach theory. It is applicable when the following conditions are satisfied [17, 18]:

- The energy of the compound nucleus has to be sufficiently high, so that almost all channels into which the nucleus can decay are dominated by integrals over the level density.
- Width fluctuations have to be negligible. This will be the case if the previous condition is satisfied.
- The transmission coefficients  $T_{\chi''I''J''}^J$  associated with the available exit channels have to be independent of the spin of the states reached in these channels. This condition is sufficiently well satisfied since the dependence of transmission coefficients on target spin is very weak.
- The level densities  $\rho_{I''}(U'')$  in the available channels have to be independent of parity and their dependence on the spin  $I''$  of the relevant nuclei has to be of the form  $\rho_{I''}(U'') \propto (2I'' + 1)$ . It can be shown that for sufficiently high energies  $U''$ , level densities are very weakly dependent on parity, so that the first of these conditions can be assumed to be satisfied. The second condition, which is a prerequisite for a rigorous derivation of the Weisskopf-Ewing limit from the full Hauser-Feshbach theory, is satisfied if the spin  $I''$  is smaller than the spin cutoff parameter  $\sigma_{cut}$  in the relevant level-density formula. In the actinide region  $\sigma_{cut} \approx 6 - 7$ , but it is known that the Weisskopf-Ewing limit is still a useful approximation at higher spins.

The Weisskopf-Ewing limit provides a simple and powerful approximate way of calculating cross sections for compound-nucleus reactions. In the context of Surrogate reactions, it greatly simplifies the application of the method: It becomes straightforward to obtain the  $J\pi$ -independent branching ratios  $\mathcal{G}_\chi^{CN}(E_{ex})$  from measurements of  $P_{\delta\chi}(E_{ex})$  and to calculate the desired reaction

cross section. Calculating the direct-reaction probabilities  $F_\delta^{CN}(E_{ex}, J, \pi)$  and modeling the decay of the compound nucleus are no longer required. However, Surrogate experiments in the Weisskopf-Ewing limit are still challenging since the requirement that both the number of  $b - \chi$  coincidences and the number of reaction events be accurately determined remains. Although the cross section expressed in Eq. 4 is differential in the outgoing-channel energy, the quantity of interest is the cross section integrated over all final-state energies. In the following, we will assume the quantity  $\mathcal{G}_\chi^{CN}$  has been integrated over the energy  $E_\chi$  of the final-state channel, and will therefore remove the differentiation with respect to energy in Eq. 4. The essential feature of this equation remains; namely, the factorization into a formation cross section and a branching ratio, neither of which depend on angular momentum or parity.

### C. The Ratio Approach

The ‘‘Ratio method’’ makes use of the Surrogate idea and requires the validity of the Weisskopf-Ewing limit. An important motivation for using the Ratio method is the fact that it eliminates the need to accurately measure  $N_\delta$ , the total number of  $d + D \rightarrow b + B^*$  reaction events, which has been the source of the largest uncertainty in Surrogate experiments performed recently. Under the proper circumstances it also reduces or removes dependence on the angular distribution of fission fragments, which is not well characterized in the present experiments.

The goal of the Ratio method is to determine the ratio

$$R(E) = \frac{\sigma_{\alpha_1\chi_1}(E)}{\sigma_{\alpha_2\chi_2}(E)} \quad (6)$$

of the cross sections of two compound-nucleus reactions,  $a_1 + A_1 \rightarrow B_1^* \rightarrow c_1 + C_1$  and  $a_2 + A_2 \rightarrow B_2^* \rightarrow c_2 + C_2$ , where the two reactions have to be ‘‘similar’’ in a sense that remains to be specified. An independent determination of one of these cross sections then allows one to infer the other by using the ratio  $R$ . In the Weisskopf-Ewing limit, the ratio  $R(E)$  can be written as:

$$R(E) = \frac{\sigma_{\alpha_1}^{CN}(E) \mathcal{G}_{\chi_1}^{CN}(E)}{\sigma_{\alpha_2}^{CN}(E) \mathcal{G}_{\chi_2}^{CN}(E)}, \quad (7)$$

with branching ratios  $\mathcal{G}_\chi^{CN}$  that are independent of  $J$  and  $\pi$  and compound-nucleus formation cross sections  $\sigma_{\alpha_1}^{CN}$  and  $\sigma_{\alpha_2}^{CN}$  that can be calculated by using an optical model.

To determine  $\mathcal{G}_{\chi_1}^{CN}/\mathcal{G}_{\chi_2}^{CN}$ , two experiments are carried out. Both use the same direct-reaction mechanism,  $D(d, b)B^*$ , but different targets,  $D_1$  and  $D_2$  to create the relevant compound nuclei,  $B_1^*$  and  $B_2^*$ , respectively. For each experiment, the number of coincidence events,  $N_{\delta_1\chi_1}^{(1)}$  and  $N_{\delta_2\chi_2}^{(2)}$ , is measured. The ratio of the branching

ratios into the desired channels for the compound nuclei created in the two reactions is given by

$$\frac{\mathcal{G}_{\chi_1}^{CN}(E)}{\mathcal{G}_{\chi_2}^{CN}(E)} = \frac{N_{\delta_1\chi_1}^{(1)}(E)}{N_{\delta_2\chi_2}^{(2)}(E)} \times \frac{N_{\delta_2}^{(2)}(E)}{N_{\delta_1}^{(1)}(E)}. \quad (8)$$

The experimental conditions are adjusted such that the relative number of reaction events,  $norm = N_{\delta_1}^{(1)}/N_{\delta_2}^{(2)}$ , can be determined by accounting for differences in beam intensities and beam times, as well as numbers of atoms in each target. This requires that the same setup be used in both experiments. The ratio of the decay probabilities then simply equals the ratio of the coincidence events and  $R(E)$  becomes:

$$R(E) = \frac{\sigma_{\alpha_1}^{CN}(E) N_{\delta_1\chi_1}^{(1)}(E)}{\sigma_{\alpha_2}^{CN}(E) N_{\delta_2\chi_2}^{(2)}(E)}, \quad (9)$$

where we have set the experimental normalization factor  $norm$  to unity.

The definition of the energy  $E$  in the above equations remains to be specified. Typically, the energy dependence of a compound-nucleus formation cross section,  $\sigma_{\alpha}^{CN} = \sigma(a + A \rightarrow B^*)$  is characterized by the kinetic energy of the projectile,  $E_{\alpha}$ , while a branching ratio is normally given as a function of the excitation energy of the compound nucleus,  $\mathcal{G}_{\chi}^{CN}(E_{ex})$ . In a compound-nucleus reaction, those two values are related via the separation energy  $S_a$  of the particle  $a$  in  $B^*$ :  $E_{ex} = S_a + E_{\alpha}$ . While either  $E_{ex}$  or  $E_{\alpha}$  can be used to uniquely specify the energy dependence of such a reaction, it is important for the Ratio method to make the comparison of the relevant reactions,  $a_1 + A_1 \rightarrow B_1^* \rightarrow c_1 + C_1$  and  $a_2 + A_2 \rightarrow B_2^* \rightarrow c_2 + C_2$  at an energy that minimizes uncertainties. Here, we take  $E$  to denote the kinetic energy of the projectile.

In Refs. [14] and [15], the Ratio method was used to obtain an estimate of the  $^{237}\text{U}(\text{n},\text{f})$  cross section. Inelastic deuteron [14] and  $\alpha$  [15] scattering experiments on  $^{238}\text{U}$  and  $^{236}\text{U}$  were carried out and fission fragments from the decay of  $^{238}\text{U}^*$  and  $^{236}\text{U}^*$  were detected in coincidence with the outgoing direct-reaction particle. The results were found to be in good agreement with a theoretical estimate by Younes *et al.* [19].

More recently, a variant of the Ratio approach described here was explored for determining the  $^{237}\text{U}(\text{n},\gamma)$  and  $^{237}\text{U}(\text{n},2\text{n})$  cross sections [20]. Rather than comparing the decay of two compound nuclei,  $B_1^*$  and  $B_2^*$ , formed with the same type of Surrogate reaction, the authors determined the ratio of decay probabilities for two *different exit channels*,  $\chi_1 = c_1 + C_1$  and  $\chi_2 = c_2 + C_2$ , of *one particular compound nucleus*,  $B_1^* = B_2^* \equiv B^*$ . This is an interesting approach that deserves further study, which is outside the scope of the present paper. We will restrict our considerations to applications of the Ratio method in which two similar compound nuclei are formed in two separate Surrogate reactions.

### III. METHOD OF THE STUDY

The purpose of the present work is an examination of the validity of the Surrogate Ratio method for determining (n,f) cross sections for actinide nuclei. In particular, we will i) use a Hauser-Feshbach-based nuclear reaction-model simulation to investigate whether the principal assumptions underlying the Ratio method are valid, and ii) employ these calculations to assess whether applying a Ratio analysis to the simulated observables yields a cross section that agrees with the expected result. While experimental tests can be very valuable, employing a simulation provides several distinct advantages: We are able to access physical quantities that are not directly observable in an experiment, such as  $J\pi$ -dependent branching ratios for a specific exit channel. We can alter quantities that are experimentally not easily modified in a controlled manner, such as the angular-momentum distribution in a compound nucleus before it decays, and carry out sensitivity studies.

For our study, we need two types of reference cross sections: The first type,  $\sigma_{\alpha_1\chi_1}$ , appears in the denominator of the ratio  $R = \frac{\sigma_{\alpha_1\chi_1}}{\sigma_{\alpha_2\chi_2}}$  and corresponds to a known cross section in real-world applications of the Ratio method. The second type of reference cross section corresponds to the unknown, “desired” cross section and serves as a benchmark for the Ratio method. We employ the full Hauser-Feshbach theory to calculate the reference cross sections relevant for our study:  $^{233}\text{U}(\text{n},\text{f})$ ,  $^{235}\text{U}(\text{n},\text{f})$ , and  $^{235\text{m}}\text{U}(\text{n},\text{f})$ . We treat the calculated  $^{233}\text{U}(\text{n},\text{f})$  cross section as the reference cross section which will appear in the denominator of the ratio  $R$ , while the  $^{235}\text{U}(\text{n},\text{f})$  and  $^{235\text{m}}\text{U}(\text{n},\text{f})$  cross sections are to be determined from a Ratio treatment. Upon extracting these by applying the Ratio prescription, we can compare the results to the reference cross sections of the second type and gain insights into the potential success of the Ratio method.

Furthermore, to simulate a Surrogate treatment, we need to generate those quantities that are typically measured in a Surrogate experiment. In particular, we need observables associated with the decay of a compound nucleus that was produced in a direct (Surrogate) reaction. Surrogate experiments focusing on (n,f) cross sections typically measure fission probabilities, while determining (n, $\gamma$ ) cross sections involves measuring gamma-ray intensities for transitions within the residual nucleus. Both fission probabilities and gamma intensities can be calculated with a Hauser-Feshbach code, such as the STAPRE code [21, 22] used in the present work. In order to account for the fact that a direct reaction produces a spin-parity distribution in the compound nucleus that is different from the spin-parity distribution associated with the desired reaction, we modified this code so that it is suitable for Surrogate-reaction studies. In particular, we included an option to allow the spin-parity distribution of the first compound nucleus to be read in from a text file rather than calculated from the entrance-channel transmission coefficients. It is therefore possible to select an

arbitrary  $J\pi$  distribution for a given compound nucleus and to predict the decay of the nucleus.

In Section IV, we will discuss various tests of the Ratio method for fission. We begin by investigating the main assumption of the method, the validity of the Weisskopf-Ewing limit, by explicitly considering the branching ratios  $G_{\chi}^{CN}(E_{ex}, J, \pi)$  of Equation 2, where  $\chi$  refers to the fission channel. In particular, we study the  $G_{\chi}^{CN}(E_{ex}, J, \pi)$  values that result from the fitting procedure of Subsection III A below, for different spin and parity values  $J\pi$  as a function of energy. We then simulate a Surrogate fission experiment. Specifically, we study fission of  $^{234}\text{U}$  and  $^{236}\text{U}$  following excitation by a direct reaction. Rather than attempting to predict the  $J\pi$  distributions that can result from the various possible direct-reaction mechanisms (transfer and inelastic reactions), we consider a few simple spin-parity distributions for  $^{234}\text{U}$  and  $^{236}\text{U}$  and observe their effect on the compound-nucleus decay. We carry out a Surrogate analysis under the assumption that the Weisskopf-Ewing limit is valid and infer the  $\sigma(^{235}\text{U}(n,f))$  and  $\sigma(^{235m}\text{U}(n,f))$  cross sections. The results are compared to the reference cross sections obtained from the full Hauser-Feshbach calculations. Furthermore, we use the fission simulation to carry out a Ratio analysis and compare the cross sections obtained in this manner to the reference cross sections. This comparison gives insight into the quality that can be achieved with the Ratio method given optimal circumstances.

### A. Nuclear-reaction model for fission

Both the calculations of the reference cross sections and the simulations of the Surrogate experiments make use of the Hauser-Feshbach statistical reaction theory. The former involve a standard Hauser-Feshbach description of the formation and decay of a compound nucleus, with parameters adjusted to reproduce available experimental data. The simulations of the Surrogate experiments employ the Hauser-Feshbach theory to describe the decay of the relevant compound nucleus only, with parameters taken from the reference-cross section calculations. The determination of the level schemes, level densities, gamma strength functions, fission-model parameters, and preequilibrium parameters is described below.

The following target nuclei are considered in our study:  $^{233}\text{U}$  which has ground-state spin and parity  $I^{\pi} = \frac{5}{2}^{+}$ ,  $^{235}\text{U}$  which has  $I^{\pi} = \frac{7}{2}^{-}$ , and  $^{235m}\text{U}$  with  $I^{\pi} = \frac{1}{2}^{+}$ . Since we are interested in neutron-induced reactions, appropriate neutron-nucleus optical potentials are needed. For simplicity, the calculations employ the same deformed neutron-nucleus optical potential for all three systems, *i.e.* the neutron transmission coefficients are independent of the target nucleus. This is a suitable approximation since the optical-model observables vary very slowly over the range of uranium isotopes considered.

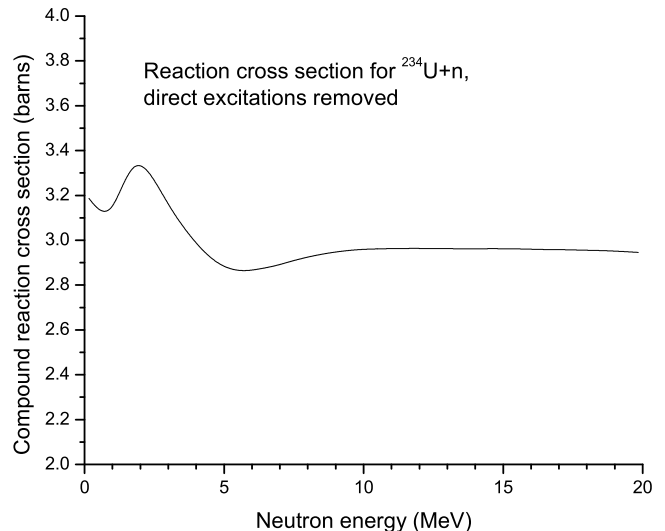


FIG. 2: Compound-nuclear cross section obtained from the Flap2.2 optical-model potential [23]. This is the reaction cross section after removal of contributions from the excitation of directly-coupled states. The calculations were carried out for neutrons incident on  $^{234}\text{U}$  and we assume  $\sigma_{n+^{234}\text{U}}^{CN} = \sigma_{n+^{235}\text{U}}^{CN} = \sigma_{n+^{235m}\text{U}}^{CN} = \sigma_{n+^{233}\text{U}}^{CN}$ .

The compound-nucleus formation cross section  $\sigma_{n+^{235}\text{U}}^{CN} = \sigma_{n+^{235m}\text{U}}^{CN} = \sigma_{n+^{233}\text{U}}^{CN}$  is plotted in Figure 2. It is expected to be accurate to approximately 5% throughout the energy range covered.

#### 1. Determining the reference cross sections

We began this study with the results of an earlier treatment of the  $^{235}\text{U}(n,2n)$  that had been carried out with the STAPRE code [24]. In this earlier calculation, level schemes, level densities, gamma strength functions, fission-model parameters, and preequilibrium parameters had been carefully adjusted to fit the available experimental data on gamma production and fission. For the present work, only small adjustments were made relative to the earlier calculation. The calculation of neutron-induced fission of  $^{233}\text{U}$  carried out for the present study proceeded in a nearly identical manner. Since we are interested in comparing reactions on the two targets, it is important that the procedures applied to both be very similar. The following remarks are applicable to both calculations.

- Level schemes and gamma branching ratios were taken from the evaluated nuclear-structure data available on the RIPL-2 web site [25]. Level densities were parameterized in the Gilbert-Cameron form [26]. The Fermi-gas parameter was fit to the observed average s-wave spacing, or obtained from the Gilbert-Cameron systematics if experimental



data were unavailable. The constant-temperature portion was constrained to reproduce the number of observed discrete levels at low energy, and matched in value and slope to the Fermi-gas form at an energy somewhat below the neutron separation energy.

- Details of the deformed optical potential (‘Flap2.2’) used in the current calculations are given in [23]; its predicted reaction cross section is shown in Fig. 2.
- Transmission coefficients for fission were calculated from the usual two-barrier model (see, for example, Bjornholm and Lynn [27]) in which the fission process proceeds through transition states built on top of the two saddle points. In the present calculations the transition states were represented by a level density; no discrete transition states were considered. For use in the fission calculations, an additional option for calculating level-densities was added to STAPRE. This option allows four constant-temperature segments, connected to a Fermi-gas form for use at energies above the constant-temperature segments. The level densities are required to be continuous at the matching points. Separate spin-cutoff parameters may be specified for the constant-temperature segments and for the Fermi-gas region. The spin-cutoff parameters used in the fits to the fission data were in the range 5–7, consistent with those in Ref. [27]. The starting values for the fission-barrier heights and curvatures were also taken from Bjornholm and Lynn [27]. These as well as the level-density parameters were varied to achieve fits to the fission cross section data.
- The gamma transmission coefficients were calculated from a standard Brink-Axel model [28, 29] using a double-humped Lorentzian parameterization of the giant dipole resonance, together with a small M1 component with a Weisskopf ( $E_\gamma^3$ ) energy dependence. Exactly the same parameters were used in all nuclei considered; the strength (peak GDR cross section) of the E1 component was adjusted to reproduce the average of the experimental values for the radiation width of the s-wave resonances in the uranium isotopes.
- Preequilibrium neutron emission in the first ( $n,n'$ ) stage of the reaction was calculated with the exciton model built into the STAPRE code. Its parameters were determined in the earlier study of reactions on  $^{235}\text{U}$  by requiring that the preequilibrium spectrum be in approximate agreement with known ( $n,n'$ ) data in the actinide region. Exactly the same parameters were used in all of the present calculations for both isotopes.
- Width-fluctuation corrections were not included in any of these calculations, nor in any of the other

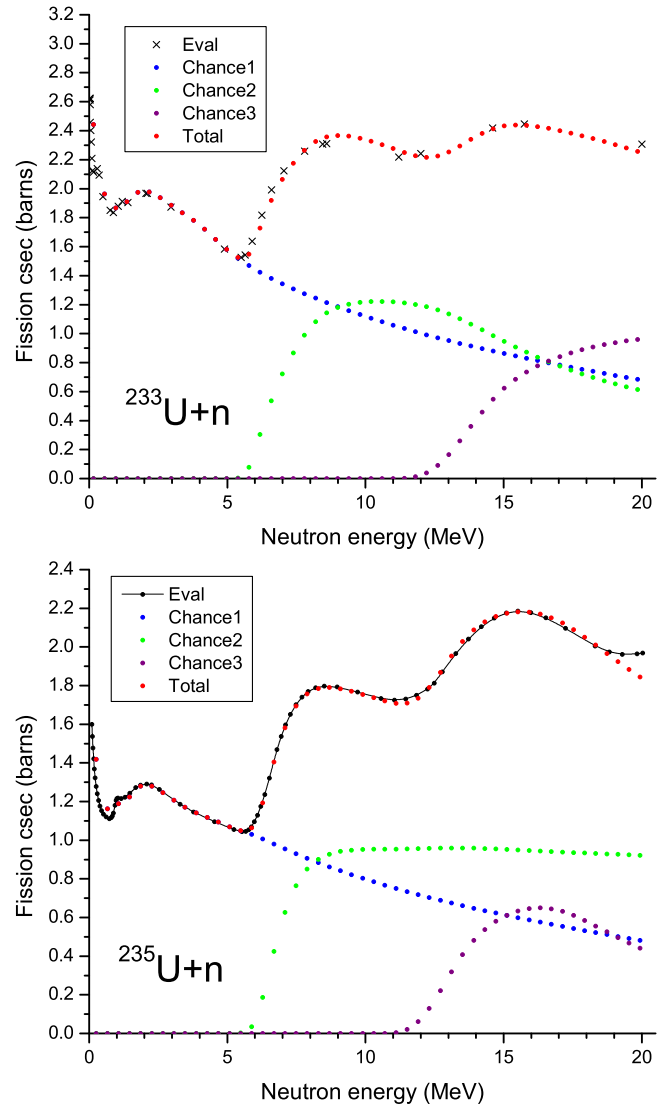


FIG. 3: Fits to the  $^{233}\text{U}$  (top panel) and  $^{235}\text{U}$  (bottom panel) fission cross sections.

results shown in this report.

The results of the fits to the fission cross sections of  $^{233}\text{U}$  and  $^{235}\text{U}$  are displayed in Fig. 3. The calculated first-, second-, and third-chance fission as well as their sum are shown, together with the evaluations to which the fission parameters were fitted. The ENDL-99 [30] evaluation and a beta version of the ENDF-7 [31] were used for  $^{235}\text{U}$  and  $^{233}\text{U}$ , respectively.

Based on the successful fit of the experimental (or evaluated) cross sections for  $^{233}\text{U}$  and  $^{235}\text{U}$ , the cross sections for reactions on the first-excited (isomeric) state of  $^{235}\text{U}$  can be predicted by changing the spin and parity of the target from  $7/2^-$  to  $1/2^+$  and keeping all other parameters fixed. The prediction for  $^{235m}\text{U}(n,f)$  is shown in Fig. 4, along with the evaluation for fission of the ground state. At the lowest energies, the cross section is lower

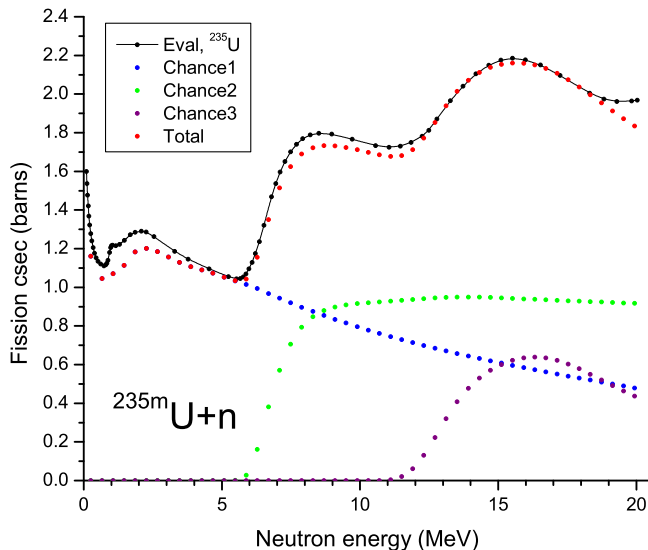


FIG. 4: Prediction of  $^{235m}\text{U}$  fission cross section using the parameters obtained from the fit to the  $^{235}\text{U}(\text{n},\text{f})$  cross section. For reference purposes, the black line shows the evaluated  $^{235}\text{U}(\text{n},\text{f})$  cross section.

than that on the ground state by about 20%. This reduction is in qualitative agreement with the results of Younes and Britt [1], even though the present calculation does not include the discrete transition states on top of the fission barriers that are believed to play a significant role in the difference between the ground and isomeric cross sections.

## 2. Simulating Surrogate experiments

In order to simulate the decay of the compound nuclei  $^{234}\text{U}$  and  $^{236}\text{U}$ , as produced in a Surrogate experiment, we employ the Hauser-Feshbach parameters determined in the fits to the  $^{233}\text{U}(\text{n},\text{f})$  and  $^{235}\text{U}(\text{n},\text{f})$  cross sections, above. We also need information on the spin-parity distributions of the decaying  $^{234}\text{U}$  and  $^{236}\text{U}$  systems. In principle, one would like to describe the direct-reaction process (transfer or inelastic scattering reaction) leading to these compound nuclei with an appropriate direct-reaction model and obtain information on the resulting  $J\pi$  distribution, which in turn can be used as input in the modified Hauser-Feshbach code. However, this is a non-trivial task since it requires a description of transfer and inelastic scattering reactions leading to unbound states, as well as an understanding of preequilibrium decay following a direct reaction (see Section III B 2 below). Moreover, a variety of projectile-target combinations with a range of possible incident energies may be considered for the direct reaction that produces the compound nucleus of interest. Different reaction mechanisms, regions of the nuclear chart, and projectile energies will yield different

compound-nuclear  $J\pi$  distributions and also provide different challenges for a proper theoretical description. For instance, for the reactions of interest here, both inelastic  $\alpha$  and deuteron scattering from actinide nuclei, as well as the  $(^3\text{He},\alpha)$  transfer reaction, have to be considered, and a proper treatment of the deformation is required. Thus, rather than focusing on obtaining a reliable prediction of the  $J\pi$  distributions that can result for these cases, we will use schematic distributions that are likely cover the range of relevant  $J\pi$  distributions.

Some guidance for selecting possible  $J\pi$  distributions can be found in the literature. One-nucleon stripping reactions, such as  $(\alpha, ^3\text{He})$ ,  $(^{20}\text{Ne}, ^{19}\text{Ne})$ , etc., with intermediate-energy projectiles,  $E \approx 20\text{--}40$  MeV/A, have received much interest in recent years. Experimental [32–34] as well as theoretical [35] work has been devoted to understanding the continuum spectra from such single-nucleon stripping reactions on spherical nuclei. In the reactions considered, relatively large angular-momentum transfers ( $l = 5, 6, 7$ ) resulted in the population of high- $j$  single-particle orbitals ( $1h_{11/2}, 1i_{13/2}, 1j_{15/2}$ , etc.), which were a major focus of those studies. Calculations for the  $^{239}\text{Pu}(\text{d},\text{p})^{240}\text{Pu}$  reaction at  $E_d = 13$  MeV [36] and for the two-nucleon stripping reaction  $(\text{t},\text{p})$  at  $E_t = 15\text{--}18$  MeV for the actinide region [1] have shown smaller angular-momentum transfers to be relevant as well. Since reactions involving targets with large ground state spins can produce compound-nuclear  $J\pi$  distributions peaked at larger angular-momentum values, it is reasonable to consider  $J > 10$  as well. Furthermore, inelastic scattering on even-even targets exhibits a characteristic asymmetry between natural and unnatural parity states: In the absence of a spin-dependent interaction only  $J^\pi = 0^+, 1^-, 2^+, \dots$  are populated (in a DWBA description). It is therefore worthwhile to study the effects of  $J\pi$  distributions that contain natural (or unnatural) parity states only.

For the purposes of the present study, we consider six different distributions. The first four, distributions a, b, c, and d, assume equal probabilities for positive and negative parity states, and are plotted in Figure 5 (top panel). These distributions have mean angular momenta  $\langle J \rangle$  of 7.03, 10.0, 12.97, and 3.30 for the curves labeled a, b, c, and d, respectively. The last two distributions, e and f, with mean angular momentum  $\langle J \rangle = 3.30$ , assume that only natural parity states ( $0^+, 1^-, 2^+$ , etc.) or only unnatural-parity states ( $0^-, 1^+, 2^-$ , etc.) are occupied, respectively, see Figure 5 (bottom panel). In Section IV, the dependence of the calculated branching ratios and extracted cross sections on the  $J\pi$  distributions of the relevant compound nucleus will be investigated using the schematic forms introduced here.

## B. The role of preequilibrium decays

Central to the Surrogate approach is the assumption that the formation and decay of the intermediate nuclear state – in both the “desired” and the Surrogate reaction

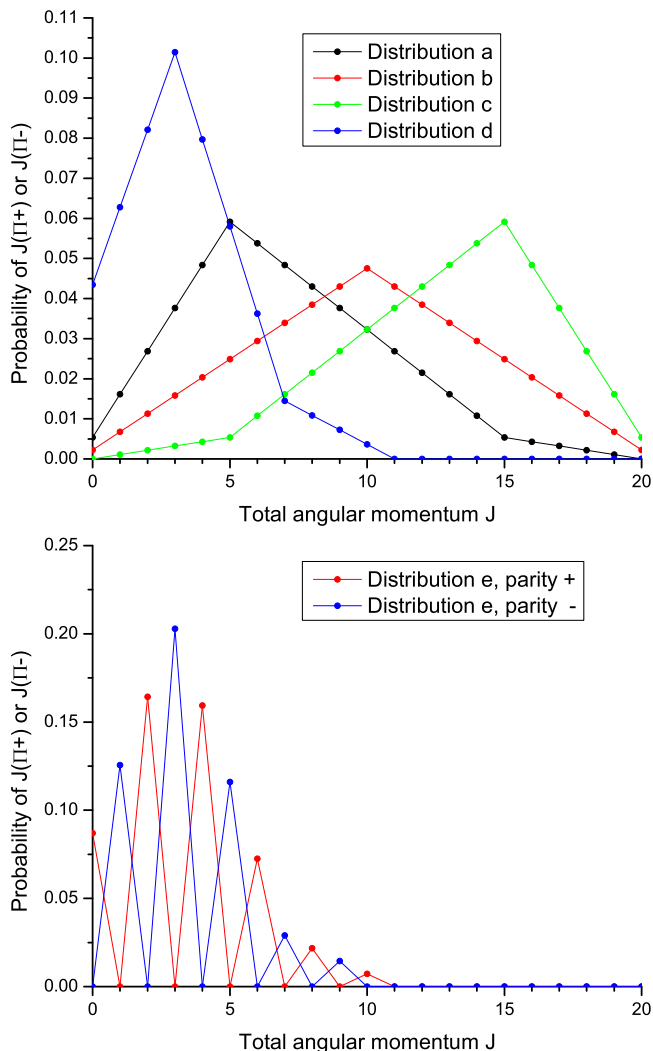


FIG. 5: Distributions of total angular momentum for the compound nuclei considered in this study. We assume that the  $J\pi$  distribution produced in a realistic Surrogate reaction falls within the range of the cases studied here. (top) Distributions a-d. The mean angular momentum is  $\langle J \rangle = 7.03, 10.0, 12.97, 3.30$  for distributions a, b, c, and d, respectively; positive and negative parities are taken to be equally probable. (bottom): Distributions e and f. Distribution e contains positive-parity states only, while distribution f contains only negative-parity states. Both have the same mean value  $\langle J \rangle = 3.30$ .

– are independent of each other (apart from conserving constants of motion). This is only valid if the intermediate nucleus equilibrates (becomes a compound nucleus) before it decays into the final reaction products.

### 1. Preequilibrium neutron emission in the desired reaction

Preequilibrium neutron emission is important for neutron-induced reactions at incident energies above a few MeV, and was therefore included in the calculations

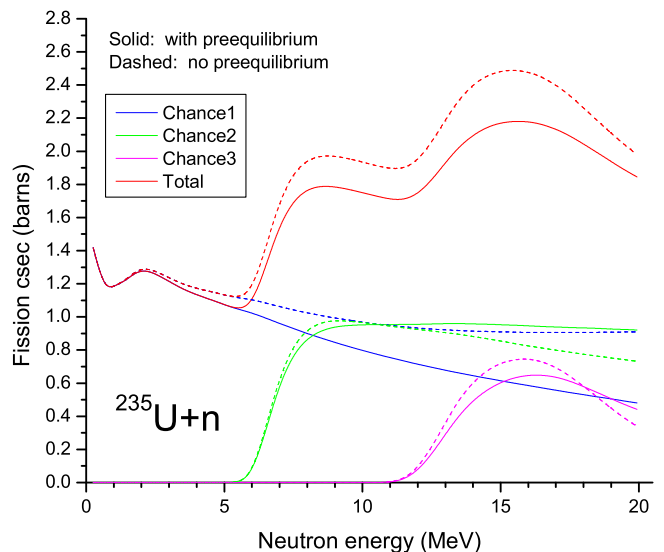


FIG. 6: The solid lines represent the fit to  $^{235}\text{U}(n,f)$  as shown in Fig. 3. The dashed lines are a calculation with identical parameters except that preequilibrium effects are turned off.

of the  $(n,f)$  cross sections described above. The Surrogate approach provides information on the decay of the desired compound nucleus and is thus not able to determine cross section contributions due to preequilibrium effects in the desired reaction. Here we consider the effects of preequilibrium emission on the  $(n,f)$  cross section. Fig. 6 shows the full calculation of the  $^{235}\text{U}(n,f)$  cross section as described earlier (solid line), together with the same calculation without preequilibrium but identical parameters otherwise (dashed line).

The principal effect of preequilibrium neutron emission is on first-chance fission; *i.e.* fission of the compound nucleus formed by fusion of the incident neutron with the target. Preequilibrium neutron emission corresponds to a fast  $(n,n')$  process that bypasses this stage and, consequently, reduces the compound-nucleus formation cross section. This is reflected in a reduction of first-chance fission, see Fig. 6. In the region where first-chance fission dominates, ( $E_n \lesssim 7$  MeV), the correction to the total fission is less than 10%. At the highest energies ( $\approx 20$  MeV), the depletion of first-chance fission is quite large, in the neighborhood of 40%. However, second- and third-chance fission are dominant in this region, so the net correction to the total fission is much less, not exceeding  $\approx 15\%$  over the entire energy range.

The effects of preequilibrium on second- and third-chance fission are much smaller than for first-chance. Although the preequilibrium  $(n,n')$  process bypasses the first compound nucleus, for sufficiently low energies of the inelastically scattered neutrons the residual nucleus will be able to undergo fission. This component of the fission cross section originates from the same residual nucleus that is reached by neutron emission from the first com-

compound nucleus, and thus must be added to the fission component (second-chance fission) arising from purely compound processes. The net result is that second- and higher-chance fission cross sections are much less sensitive to the inclusion of preequilibrium than the first-chance process.

In principle, it is necessary to independently determine preequilibrium corrections to the cross sections extracted from a Surrogate analysis. We do not determine such corrections in our current study. For the cases considered here, the total fission cross sections calculated with and without preequilibrium were found to be within 15% of each other. Moreover, we expect that the corrections for preequilibrium should be very similar for targets differing only by two neutrons ( $^{233}\text{U}(n,f)$  vs.  $^{235}\text{U}(n,f)$ ) as studied here, or  $^{235}\text{U}(n,f)$  vs.  $^{237}\text{U}(n,f)$  as presently being inferred from experiments using the Ratio method [14, 15]). Therefore, the errors incurred by omitting preequilibrium corrections are likely to be significantly smaller than 15% when the Ratio method is used.

## 2. Preequilibrium decay in the Surrogate reaction

The objective of a Surrogate reaction  $d + D \rightarrow b + B^*$  is the production of a compound nucleus  $B^*$ , the decay of which we observe experimentally. In order to infer useful information on the desired decay probabilities, one needs to be sure that the observed quantities (such as  $b$ -fission coincidence events) are indeed associated with the desired nucleus  $B^*$  and that this nucleus was in statistical equilibrium before the decay.

Experimentally, it is often not possible to verify this: fission fragments might originate from the desired compound nucleus or from a neighboring nucleus, the intermediate nucleus might have decayed before reaching equilibrium, etc. A theoretical assessment is also difficult, since it requires a thorough understanding of the process by which the desired compound nucleus is formed. For example, inelastic scattering can excite a target nucleus by producing one-particle one-hole (1p-1h) states, which can evolve to 2p-2h, 3p-3h, etc., configurations and eventually to a compound nucleus. At any stage it is possible that a particle escapes, thus preventing the formation of the desired compound nucleus. For a stripping reaction, one has to disentangle the contribution from various processes, such as breakup, breakup-fusion, and direct stripping to resonances, and determine the probability that the relevant resonance state evolves to produce a compound nucleus. Moreover, it is not sufficient to estimate the probability of preequilibrium decay for a given Surrogate reaction, one also needs to determine its effect on the  $J\pi$  distribution of the desired nucleus. It is expected that preequilibrium decay proceeds predominantly through particular  $J\pi$  states, *i.e.* the  $J\pi$  distribution of the decaying compound nucleus is likely to be different from the distribution that was present immediately following the direct-reaction process.

The model employed here does not make any statements or assumptions about possible preequilibrium effects in the Surrogate reaction. It starts with a given compound nucleus and  $J\pi$  distribution and follows the decay of that nucleus in the Hauser-Feshbach framework. The process of producing a particular  $J\pi$  distribution for a given compound nucleus via a direct reaction deserves additional attention in a more complete treatment of Surrogate reactions. This is outside the scope of the present study.

## IV. SURROGATE METHODS FOR FISSION

For this study we carry out various tests relevant to the Surrogate method in the Weisskopf-Ewing limit and the Ratio method. We focus on applications to neutron-induced fission. First, we calculate branching ratios for fission as a function of the spin and parity of the initially formed compound nucleus. We then study the validity of the Surrogate method for calculating fission cross sections for individual nuclei using the Weisskopf-Ewing assumption. This is done by comparing the predictions of the method with the reference cross sections calculated from the full Hauser-Feshbach theory, as outlined in the previous section. Finally, we study the validity of the Ratio method by the same technique. Our findings are presented below.

### A. Branching Ratios and the Weisskopf-Ewing Assumption

The branching ratios  $G_{\chi=fission}^{CN}(E_{ex}, J, \pi)$  defined in Eq. 2 are independent of the spin and parity values  $J\pi$  if the Weisskopf-Ewing limit of the full Hauser-Feshbach theory is applicable. While these branching ratios cannot be directly measured in a fission experiment, they can be extracted from a calculation of the (n,f) cross section and their  $J\pi$ -dependence can be studied. This allows us to assess the validity of the Weisskopf-Ewing assumption.

In our calculation the branching ratio for one particular  $J\pi$  combination is obtained as follows: First, all parameters (level densities, gamma strength functions, fission-model parameters, etc.) of the Hauser-Feshbach-plus-preequilibrium calculation are determined as outlined in Section III A 1. Since the modified STAPRE code allows one to calculate the quantity  $\sum_{J,\pi} f^{CN}(E_{ex}, J, \pi) G_{\chi}^{CN}(E_{ex}, J, \pi)$ , where  $f^{CN}(E_{ex}, J, \pi)$  is an arbitrary  $J\pi$  distribution in the compound nucleus, we can set  $f^{CN}(E_{ex}, J, \pi) = 1$  for a particular  $(J, \pi)$  value  $(J_0, \pi_0)$ , and zero otherwise. This allows us to obtain the individual branching ratios,  $G_{\chi=fission}^{CN}(E_{ex}, J_0, \pi_0)$ , samples of which are plotted in Figures 7–9. Note that the results shown are the actual branching ratios (*i.e.* fission probabilities) that are used in the full calculation of the (n,f) cross section.

Figure 7 gives the  $G_{\chi}^{CN}(E_{ex}, J, \pi)$  for the  $^{233}\text{U}(n,f)$  reaction for fission proceeding through positive and negative parity states of the compound nucleus  $^{234}\text{U}$ . We observe that the branching ratios exhibit a significant  $J\pi$  dependence. In particular, for low energies,  $E_n = 0 - 5$  MeV (where  $E_n$  is the energy above the neutron separation energy in the compound nucleus;  $E_n = E_{ex}(^{234}\text{U}) - S_n$ , corresponding to the energy of the incoming neutron in the desired (n,f) reaction), the  $G_{fission}^{CN}(E_{ex}, J, \pi)$  differ in both their energy dependence and their magnitude for different  $J\pi$  values. We find variations as large as a factor two in absolute value. With increasing energy, the differences decrease, although the discrepancies become more pronounced as the thresholds for second-chance and third-chance fission of  $^{234}\text{U}$  are crossed, at  $\approx 6$  MeV and  $\approx 13$  MeV, respectively. For energies above 5 MeV, the differences are at most 25-30%. Comparing the top and bottom panels of Figure 7, we also note that the dependence of the  $G_{fission}^{CN}(E_{ex}, J, \pi)$  on parity is much smaller than the angular-momentum effect. It is clear that for low energies (below 2 MeV) the Weisskopf-Ewing approach is not a good approximation, while the energy regime above 5 MeV merits further study.

Figure 8 shows the branching ratios for the  $^{235,235m}\text{U}(n,f)$  reactions for positive and negative parity states in the compound nucleus  $^{236}\text{U}$ . We find trends similar to those exhibited by the previous case. The discrepancies are more pronounced in this case than in the  $^{234}\text{U}$  example, with differences of up to a factor three in the absolute values. Here as well, the  $G_{fission}^{CN}(E_{ex}, J, \pi)$  become more alike with increasing energy except near the thresholds for second-chance and third-chance fission.

The calculations demonstrate that the validity of the Weisskopf-Ewing approximation depends on the range of  $J\pi$  values that play a role in the decay of the compound nucleus. While it may be possible to apply the Weisskopf-Ewing approximation to a reaction that populates a narrow range of  $J\pi$  states, this description will break down for cases which involve a wide range of angular-momentum values. For example, for reactions that populate only the  $J = 0, \dots, 4$  states in  $^{236}\text{U}$  it is reasonable to expect the Weisskopf-Ewing approximation to provide a valid description of fission of  $^{236}\text{U}$ , at equivalent neutron energies above  $E_n \approx 1.0$  MeV (see Figure 9). On the other hand, if the states that are populated in the compound nucleus before the decay have large angular momenta ( $J \gtrsim 5$  here), the condition  $J \lesssim \sigma_{cutoff}$  required for the Weisskopf-Ewing limit to be a good approximation to the Hauser-Feshbach theory is no longer satisfied and the branching ratios may depend on  $J\pi$ . It is therefore worthwhile to not only study the dependence of the branching ratios on the spin and parity of the decaying nucleus, but also to develop and test theories that allow for a prediction of the  $J\pi$  populations of a compound nucleus following a variety of possible direct reactions.

The findings here illustrate an important point: Restricting one's consideration to reactions induced by neu-

trons with kinetic energies above several MeV does not guarantee the validity of the Weisskopf-Ewing limit. The validity of this approximation depends clearly on the energy of the compound nucleus as well as on the range of  $J\pi$  values that play a role in the decay of the compound nucleus. Angular-momentum values larger than the spin cutoff factor invalidate the Weisskopf-Ewing assumption, and we have seen that this assumption also breaks down near the threshold for second-chance and, to a lesser degree, third-chance fission. We have to conclude that it is not *a priori* clear whether the Weisskopf-Ewing limit applies to a particular reaction in a given energy regime. This needs to be verified for each case of interest.

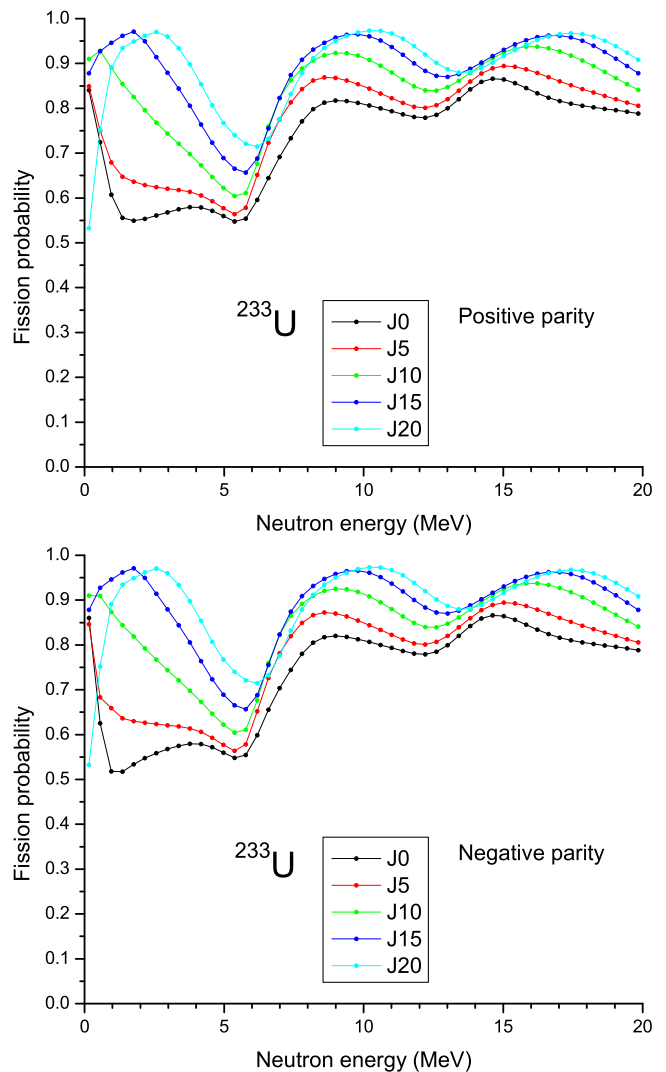


FIG. 7: Calculated branching ratios  $G_{fission}^{CN}(E_{ex}, J, \pi)$  for neutron-induced fission on  $^{233}\text{U}$ . Results are shown for positive (top panel) and negative (bottom panel) parity states with total angular momenta  $J = 0, 5, 10, 15, 20$  in the compound nucleus  $^{234}\text{U}^*$ .

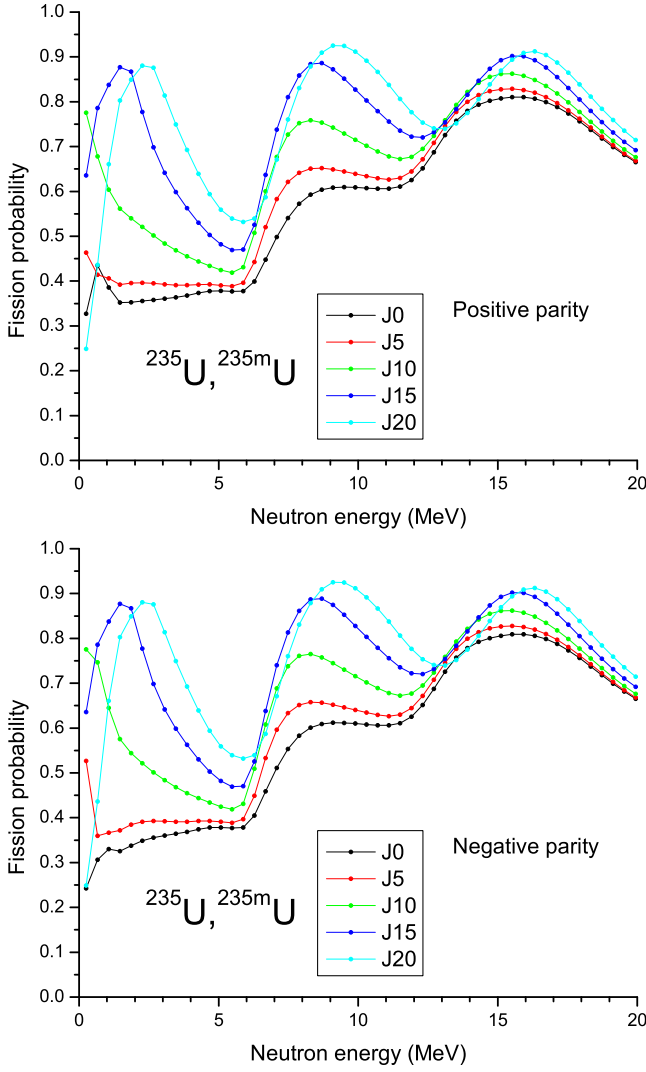


FIG. 8: Calculated branching ratios  $G_{fission}^{CN}(E_{ex}, J, \pi)$  for neutron-induced fission on  $^{235}\text{U}$  and  $^{235m}\text{U}$ . Results are shown for positive (top panel) and negative (bottom panel) parity states with total angular momenta  $J = 0, 5, 10, 15, 20$  in the compound nucleus  $^{236}\text{U}^*$ .

### B. Simulated Surrogate Fission Cross Sections in the Weisskopf-Ewing Approximation

Using the branching ratios discussed in the previous subsection we can now simulate a Surrogate fission experiment. While the individual branching ratios  $G_{\chi}^{CN}(E_{ex}, J, \pi)$  do not depend on the formation mechanism for the compound nucleus, the measured decay probabilities  $P_{\chi}(E_{ex}) = \sum_{J, \pi} f^{CN}(E_{ex}, J, \pi) G_{\chi}^{CN}(E_{ex}, J, \pi)$  depend on the relative weights  $f^{CN}(E_{ex}, J, \pi)$  which in turn are determined by the process that formed the compound nucleus. For example,  $f^{CN}(E_{ex}, J, \pi) = \sigma_{n+A}^{CN}(E_{ex}, J, \pi) / \sum_{J', \pi'} \sigma_{n+A}^{CN}(E_{ex}, J', \pi')$  for the

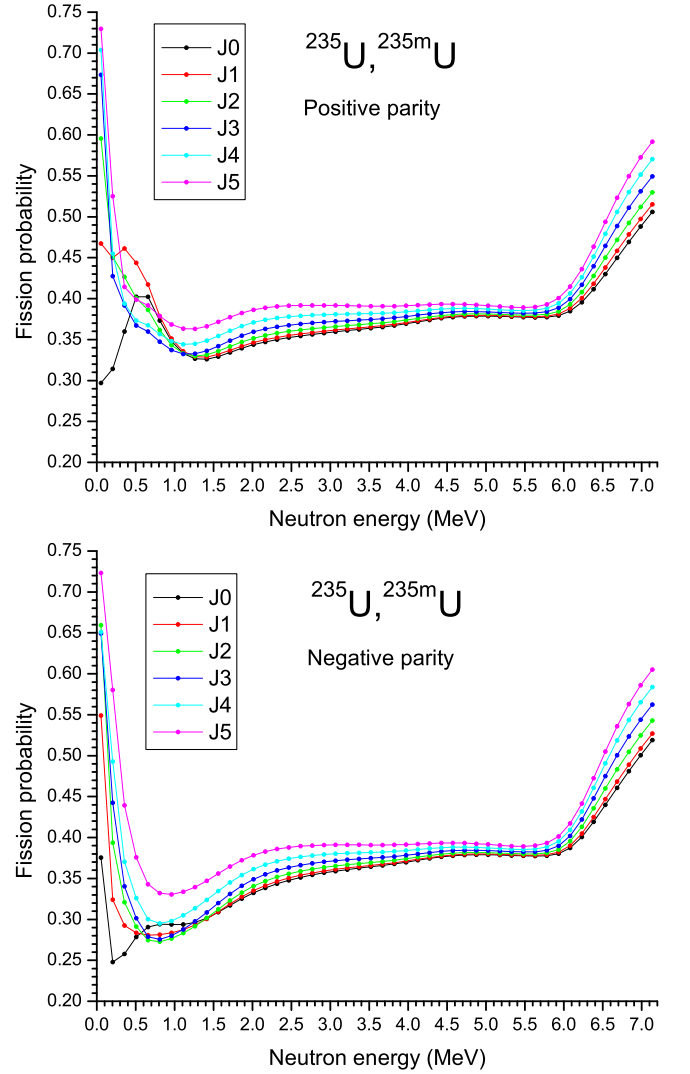


FIG. 9: Same as in Figure 8, but for small total angular momenta,  $J = 0, 1, 2, 3, 4,$  and  $5$ , of the compound nucleus  $^{236}\text{U}^*$ .

neutron-induced reaction  $n + A \rightarrow B^*$ , where  $\sigma_{n+A}^{CN}(E_{ex}, J, \pi)$  is the cross section for forming the compound nucleus at energy  $E_{ex}$  with angular momentum  $J$  and parity  $\pi$ . On the other hand,  $f^{CN}(E_{ex}, J, \pi) = F_{\delta}^{CN}(E_{ex}, J, \pi)$  for a Surrogate reaction,  $\delta = d + D \rightarrow b + B^*$ , is determined by the relative direct-reaction cross sections for the individual  $J\pi$  values.

In our simulation of a Surrogate reaction, we consider six possible distributions (shown in Figure 5) for the weights  $F_{\delta}^{CN}(E_{ex}, J, \pi)$  and investigate their effect on the extracted (n,f) cross sections. With the help of the modified STAPRE code we determine

$$P_{\delta\chi}^{(p)}(E_{ex}) = \sum_{J, \pi} F_{\delta}^{CN(p)}(E_{ex}, J, \pi) G_{\chi}^{CN}(E_{ex}, J, \pi), \quad (10)$$

where  $\chi = fission$ , which simulates an experimentally observable  $b$ -fission coincidence probability, for each of the selected compound-nuclear  $J\pi$  populations,  $p = a, \dots e$ . These distributions are normalized so that their sum over all  $J$  and  $\pi$  values is unity. We then calculate the desired fission cross section,

$$\sigma_{(n,f)}^{WE(p)}(E_{ex}) = \sigma_{n+A}^{CN}(E_{ex}) \mathcal{G}_{fission}^{CN(p)}(E_{ex}), \quad (11)$$

assuming  $J\pi$ -independent branching ratios  $\mathcal{G}_{fission}^{CN(p)}(E_{ex}) = P_{\delta\chi}^{(p)}(E_{ex})$ . This procedure corresponds to a Surrogate analysis in the Weisskopf-Ewing approximation of the simulated ( $d + D \rightarrow b + B^* \rightarrow b + fission$ ) experiment, since in this limit, we have  $P_{\delta\chi} = \mathcal{G}_{fission}^{CN} \times \sum_{J,\pi} F_{\delta}^{CN}$  and, as noted above,  $\sum_{J,\pi} F_{\delta}^{CN} = 1$ . The compound-nucleus formation cross section  $\sigma_{n+A}^{CN}(E_{ex})$  is taken to be the one shown in Figure 2.

The deduced (n,f) cross sections for a given target nucleus and  $J\pi$  distribution  $p$  can then be compared to the calculated reference cross sections obtained as described in Section III A 1. In particular, the extracted cross sections should not depend on the  $J\pi$  distribution chosen if the Weisskopf-Ewing limit is a good approximation. However, given the findings presented above, we should not be surprised to find that the cross sections obtained in the manner described differ significantly from each other as well as from the reference cross sections, particularly for energies lower than 5 MeV and high compound nucleus spins.

Results for the  $^{233}\text{U}(n,f)$  cross section deduced from simulated Surrogate experiments are shown in Figure 10 (top panel). Cross sections obtained for the four  $J\pi$  distributions  $p = a, b, c,$  and  $d$  are given, along with the reference cross section for this reaction. Cross sections obtained for distributions  $e$  and  $f$  are almost identical to the result for  $p = d$  and are not plotted. We observe that the inferred cross sections for  $p = a, b,$  and  $c$  are too large, by up to 15-20% for energies above 5 MeV and up to 50% for smaller energies, while the results for  $p = d, e,$  and  $f$  are within 10% of the expected cross section for all energies considered. The deduced cross sections clearly depend on the  $J\pi$  distribution considered for the compound nucleus. This reflects the fact that the Weisskopf-Ewing limit is not strictly valid in this case. The uncertainties are particularly large for energies below 3 MeV, as expected given the findings of Section IV A. For energies  $E_n \approx 0 - 5$  MeV, the extracted cross section for distribution  $d$  is in excellent agreement with the reference cross section, since in this energy range the  $J\pi$  population of the compound nucleus  $^{236}\text{U}$ , as produced in the neutron +  $^{235}\text{U}$  fusion process is similar to distribution  $d$ , see Figure 11. Identifying a Surrogate reaction that produces a compound nucleus similar to the one produced in the desired reaction obviously yields the best results for the extracted cross section.

The bottom panel of Figure 10 shows similar results for the extracted  $^{235}\text{U}(n,f)$  and  $^{235m}\text{U}(n,f)$  cross sections. Note that the results are the same for both cases since

we simulate the Surrogate reaction with the same six possible  $J\pi$  distributions and we assume the compound nucleus formation cross section to be independent of the target nucleus for the range of uranium isotopes studied here. Here as well, we find that the results for distribution  $d, e,$  and  $f$  are almost undistinguishable and we plot only the cross section extracted for  $p = d$ . The findings are similar to those for the  $^{233}\text{U}$  case, but the discrepancies between the different curves are more pronounced here. For distributions  $p = a, b,$  and  $c$ , the Surrogate analysis overestimates the cross sections by as much as 40% for energies larger than 5 MeV and a factor 2.5 in the low-energy regime. For distributions  $p = d, e,$  and  $f$ , we find that the extracted cross sections are in very close agreement with the expected results for  $E_n = 0 - 8$  MeV and too large by about 10-15% for larger energies. The influence of the spin-parity distribution in the compound nucleus on the extracted cross sections is significant; again, this reflects the fact that the Weisskopf-Ewing approximation is deficient at low energies (below about 3 MeV) when not enough channels are open and at higher energies when the spin-parity distribution extends to values significantly higher than the spin-cutoff parameter in the level densities in the decay channels. While the extracted cross sections are least sensitive to the underlying  $J\pi$  distributions in the energy range  $E_n = 13 - 20$  MeV, they overestimate the cross section by 10-15%. These discrepancies are primarily due to preequilibrium effects, which reduce the reference cross section (see Section III B and Figure 6), and are not included in the type of Surrogate reaction measurements simulated here.

### C. Simulation of the Ratio Method for Fission

We are now in a position to carry out a Ratio analysis, using results from the simulated Surrogate experiments  $d + D \rightarrow b + B^* \rightarrow b + \chi$  in which the compound nuclei  $^{234}\text{U}$  and  $^{236}\text{U}$  decay by fission. As explained in detail in Section II C, the Ratio method makes use of the Surrogate idea and assumes the validity of the Weisskopf-Ewing limit. While a Surrogate analysis in the Weisskopf-Ewing approximation requires that one determine the absolute probabilities  $P_{\delta\chi} = \mathcal{G}_{\chi}^{CN}$  for the decay channel of interest ( $\chi = fission$  in the current case), for the Ratio method it is sufficient to determine the relative probabilities in order to relate the unknown desired cross section  $\sigma_{\alpha_1\chi_1}$  to a known cross section  $\sigma_{\alpha_2\chi_2}$  via Equation 6.

In this study we treat the reference cross section  $\sigma(^{233}\text{U}(n,f))$  as the known cross section and  $\sigma(^{235}\text{U}(n,f))$  as the unknown desired cross section. We have

$$R(E) = \frac{\sigma_{n+^{235}\text{U}}^{CN}(E) \mathcal{G}_{^{236}\text{U}^* \rightarrow f}^{CN}(E)}{\sigma_{n+^{233}\text{U}}^{CN}(E) \mathcal{G}_{^{234}\text{U}^* \rightarrow f}^{CN}(E)} = \frac{\mathcal{G}_{^{236}\text{U}^* \rightarrow f}^{CN}(E)}{\mathcal{G}_{^{234}\text{U}^* \rightarrow f}^{CN}(E)} \quad (12)$$

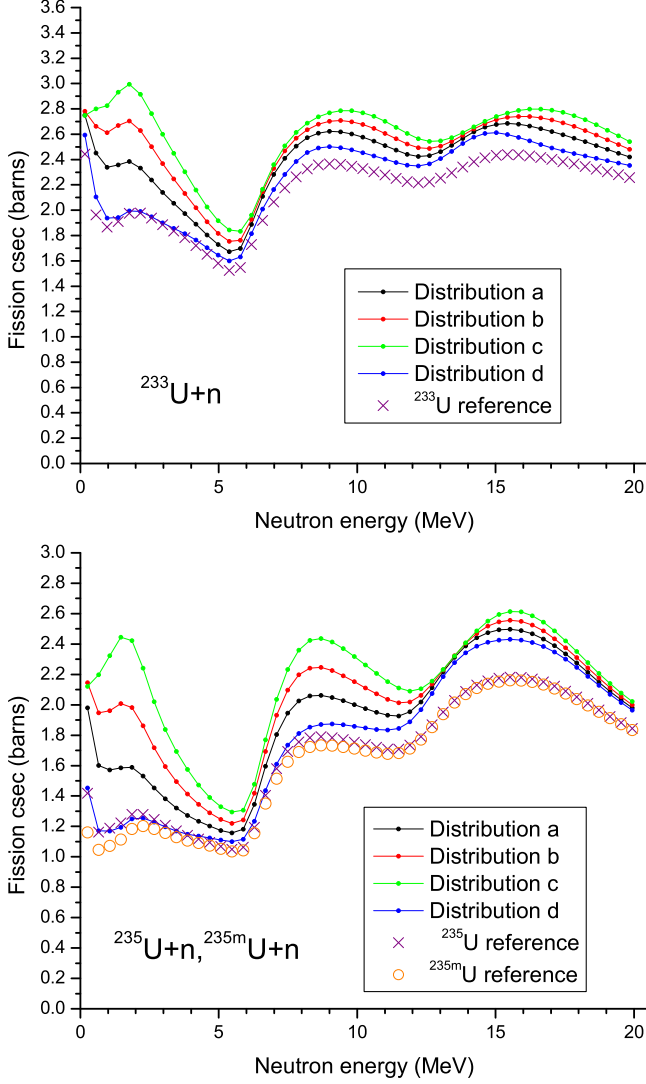


FIG. 10: Weisskopf-Ewing estimates for (n,f) cross sections, using different estimates for the distribution of angular momenta in the initial compound nucleus, compared to the calculated reference cross section. The latter were obtained from a careful adjustment of a complete (n,f) calculation. (Top panel) Estimated and expected cross sections for  $^{233}\text{U}(n,f)$ . The crosses represent the  $^{233}\text{U}(n,f)$  reference cross section. (Bottom panel) Estimated and expected cross sections for  $^{235}\text{U}(n,f)$  and  $^{235m}\text{U}(n,f)$ . The crosses represent the  $^{235}\text{U}(n,f)$  reference cross section and the circles represent the reference cross section for  $^{235m}\text{U}(n,f)$ . In both cases, the results for distributions e and f are almost identical to the cross section extracted for distribution d and are not shown.

since  $\sigma_{n+^{233}\text{U}}^{CN} = \sigma_{n+^{235}\text{U}}^{CN}$  here. The branching ratios are those shown in Figures 7–9. For each  $J\pi$  distribution considered,  $p = a, \dots, f$  we determine the ratio  $R^{(p)}(E)$  from the associated probabilities  $P_{\delta\chi}^{(p)}$  and deduce the desired cross section  $\sigma^{(p)}(^{235}\text{U}(n,f)) = R^{(p)} \times \sigma(^{233}\text{U}(n,f))$ . We carry out such an analysis for both the ground state,

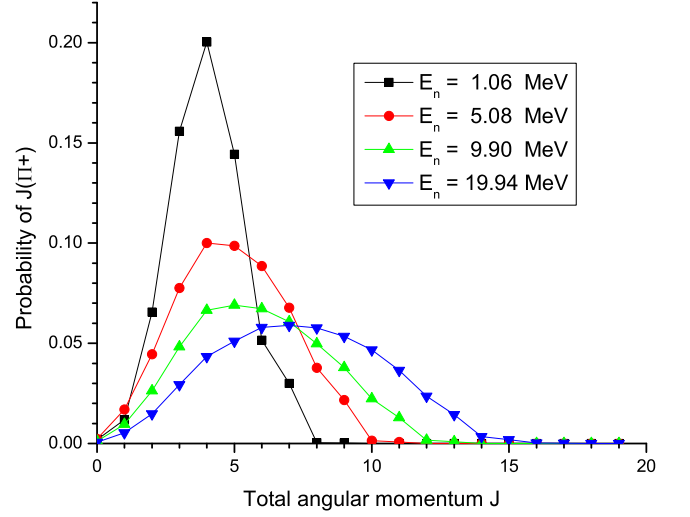


FIG. 11: Angular-momentum distribution of positive-parity states of the compound nucleus  $^{236}\text{U}$ , following neutron absorption by  $^{235}\text{U}$ , for various neutron energies. The negative-parity distribution is qualitatively similar.

$^{235}\text{U}$ , and the unstable first excited state,  $^{235m}\text{U}$ , of the target nucleus. Since both  $^{235}\text{U}(n,f)$  and  $^{235m}\text{U}(n,f)$  proceed through the same compound nucleus,  $^{236}\text{U}$ , the comparison of the two cases will provide insight into the role of the target spin in the neutron-induced reactions.

The (n,f) cross sections deduced from the Ratio analysis of the simulated Surrogate experiments are shown in Figure 12 for  $^{235}\text{U}(n,f)$  (top panel) and  $^{235m}\text{U}(n,f)$  (bottom panel). In each case, the inferred cross section is compared to the calculated reference cross section.

We observe that the  $J\pi$  distributions,  $p = a, \dots, f$  have a much smaller effect on the cross sections deduced here than on the cross sections obtained from a Surrogate analysis in the Weisskopf-Ewing limit; *i.e.* the Ratio method is less sensitive to the details of the spin-parity distributions.

For both examples, we find relatively good agreement between the simulated Ratio results and the expected cross sections for energies above about 3 MeV. The largest discrepancies, which may be as large as 50%, occur where the Weisskopf-Ewing approximation is no longer valid, *i.e.* at small energies ( $E_n \leq 3$  MeV) and for angular-momentum distributions with high average  $J$  values. We also find differences of up to about 25% near the threshold for second-chance fission. At the same time, the cross sections associated with distribution d are in excellent agreement with the expected results for energies up to about 7-8 MeV, where preequilibrium effects set in. Overall, the agreement is slightly better for the  $^{235}\text{U}$  target than for the  $^{235m}\text{U}$  case.

For situations in which the Weisskopf-Ewing limit provides at least a rough approximation, *e.g.* for  $E_n = 5$ –20 MeV in the cases considered here, the Ratio method further reduces the discrepancies between the extracted and



expected cross sections, thus providing significantly improved results. Effects that, in the Surrogate Weisskopf-Ewing approach, cause deviations from the correct results seem to affect the  $^{235,235m}\text{U}(n,f)$  and  $^{233}\text{U}(n,f)$  cross sections in a similar manner and hence cancel in part in the Surrogate Ratio treatment. This is in particular notable for the preequilibrium decays, the effects of which were pronounced in the Weisskopf-Ewing approach and are significantly smaller here.

Despite the apparent success of the Ratio treatment, there remains a dependence on the form of the initial spin-parity distribution in the compound nucleus, which is not well known at this time. It would be helpful to have realistic calculations and experimental data that allow one to place constraints on the possible compound-nucleus  $J\pi$  distributions. Some information on the spins of a compound nucleus decaying via the emission of  $\gamma$  rays can in principle be inferred from a measurement of the  $\gamma$ -ray intensities. This will be the subject of a separate study.

#### D. Fission Fragment Angular Distributions and Surrogate Analyses

Nuclear fragments resulting from fission of a nucleus  $B^*$  that has been excited in a direct reaction, such as a transfer reaction or an inelastic excitation, are in general not isotropically distributed. This then implies that it is not straightforward to infer the total number of fission fragments from a realistic experiment in which the fission detectors cover only a portion of  $4\pi$ . In a Surrogate reaction, fission fragments are detected in coincidence with the outgoing particle from the direct reaction.

Angular correlations between the outgoing direct-reaction particle and fission fragments were studied in the 1960s for (d,pf), (t,pf), (t,df), and ( $\alpha$ ,  $\alpha'$ f) reactions [37–43]. For a given projectile-target combination, the distributions  $W(\theta, \phi)$  were found to depend on a variety of parameters: i) the energy  $E^*$  to which the nucleus  $B^*$  was excited in the direct reaction; ii) properties of the transition states populated in  $B^*$ , such as the parity  $\pi$  of the relevant state, as well as the angular-momentum  $J$  and its projections  $K$  and  $M$  on the body-fixed and laboratory-fixed axes, respectively; iii) the angle  $\psi$  of the outgoing direct-reaction particle with respect to the beam direction. Both the stripping and the inelastic scattering studies found the anisotropies in the fission fragment distribution to be particularly large near the fission threshold. In fact, the dependence of the angular distribution near the fission barrier on the  $J, K, M$ , and  $\pi$  quantum numbers of the transition states was exploited to study the structure of these states.

These findings imply that for a proper application of the Surrogate method, the angular correlations have to be known. A detailed description of the spatial anisotropies is required if one needs to determine the total number of fission fragments from a measurement at a

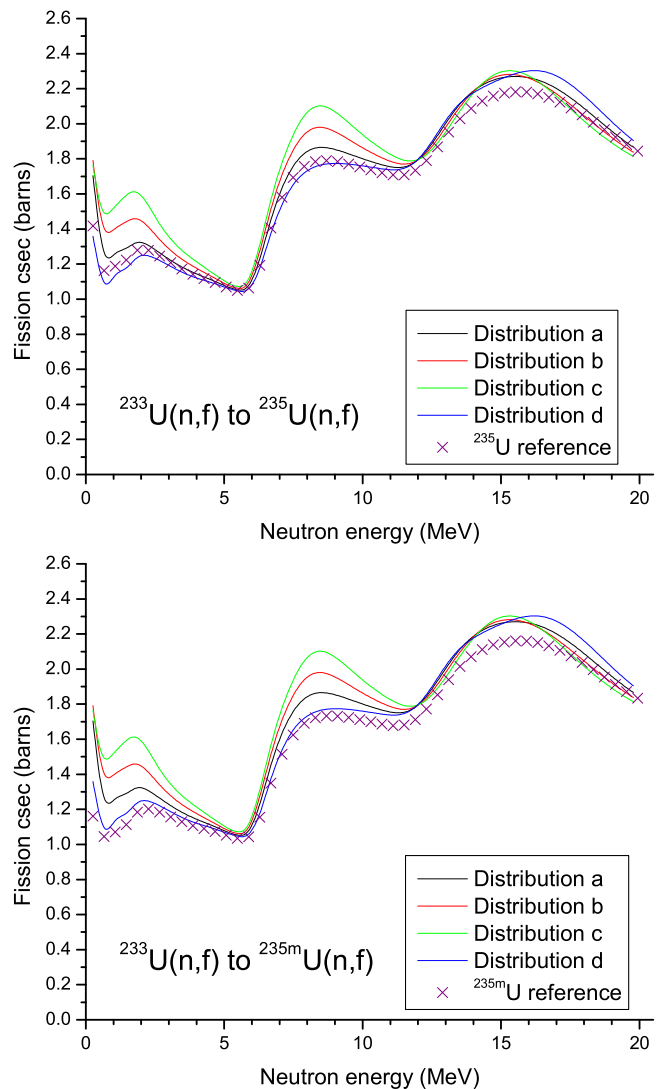


FIG. 12: Estimates of the  $^{235}\text{U}(n,f)$  (top panel) and  $^{235m}\text{U}(n,f)$  (bottom panel) cross sections obtained from the Ratio method, using different estimates for the distribution of angular momenta in the initial compound nucleus. Distributions e and f yield results very similar to those for case d and are not shown. The crosses represent the reference cross sections as obtained in Section III A 1.

particular location in space. Petit *et al.* [13], in a recent Surrogate experiment, measured angular distributions of fission fragments and accounted for the anisotropies explicitly.

Alternatively, it might be possible to carry out the fission fragment measurements in coincidence with the outgoing direct-reaction particle at an angle that is associated with only minor anisotropies in the fission-fragment distribution. The latter strategy was followed by Cramer and Britt [8], who detected outgoing protons from (t,pf) reactions on several actinide targets at back angles in order to minimize the effects of the angular correlations on

their results. It is not obvious that such angles can be found for all cases of interest.

Similarly, knowledge of the angular correlations is important for a successful application of the Ratio method. The two strategies outlined above for Surrogate applications, correcting the measured fission counts or restricting the coincidence measurements to selected angles for the direct-reaction particle, can be pursued here as well. However, the treatment of the anisotropies greatly simplifies in the Ratio approach when the angular correlations for the two compound nuclei that are being compared are very similar. In this case, the ratio of the angular distribution functions for the two nuclei can be approximately set to unity, as was seen in Ref. [15].

## V. SUMMARY AND CONCLUSIONS

We have examined the validity of the Surrogate Ratio method for determining (n,f) cross sections for actinide nuclei. The study was motivated by recent (d,d') and ( $\alpha,\alpha'$ ) Surrogate experiments at Yale [14] and Berkeley [15], respectively, that were analyzed in the framework of the Ratio approach. Both experiments determined the ratio  $\sigma(^{237}\text{U}(n,f)) / \sigma(^{235}\text{U}(n,f))$ , which made it possible to obtain the (n,f) cross section for the short-lived ( $\tau_{1/2} = 6.8\text{d}$ ) isotope  $^{237}\text{U}$  [14, 15, 44], since the  $^{235}\text{U}(n,f)$  cross section was already known. We investigated the assumptions underlying the Ratio method and carried out simulations to assess whether the cross sections that are obtained indirectly by applying the Ratio method agree with the expected results.

More specifically, we carried out statistical calculations for (n,f) reactions on  $^{233}\text{U}$ ,  $^{235}\text{U}$ , and  $^{235m}\text{U}$  targets and examined the resulting fission branching ratios. We found the individual fission branching ratios  $G_{fission}^{CN}(E, J, \pi)$  to be clearly dependent on the  $J\pi$  values of the compound-nuclear states. Both the energy of the decaying compound nucleus as well as the range of angular momentum (and parity) values of the states populated in the reaction place limitations on the validity of the Weisskopf-Ewing approximation.

We simulated physical quantities that can be measured in a Surrogate experiment and carried out a Surrogate analysis that made use of the Weisskopf-Ewing approximation. The extracted cross sections were seen to deviate from the expected reference cross sections by up to 40% for neutron energies above 5 MeV, and larger deviations, as much as a factor of 2.5, were found at lower energies. For energies below about 10 MeV, the discrepancies between the inferred and reference cross sections can to a large extent be attributed to the differences in the spin-parity distributions. The effect is particularly striking for the energy regime  $E_n \approx 0\text{-}3$  MeV. Preequilibrium effects, which were included in the reference cross sections, but not in the simulated Surrogate reactions, were seen to contribute to the deviations at higher energies ( $E_n \gtrsim 13$  MeV).

We also applied a Ratio analysis to the simulated physical quantities and compared the results to the reference cross sections. The fission cross sections inferred in this manner were found to be in much better agreement with the expected results than the cross sections inferred from the previous (Surrogate Weisskopf-Ewing) analysis. The Ratio analysis yielded deviations less than 50% at low energies ( $E_n \approx 0\text{-}3$  MeV) and no more than 25% for the larger energies investigated. Variations in the  $J\pi$  distributions had a much smaller effect on the extracted cross section and the deviations due to preequilibrium effects were diminished as well.

It needs to be emphasized that these findings apply to the Ratio analyses of the experiments simulated here. In actual experiments, additional uncertainties are introduced, *e.g.* determining the total number of fission fragments requires, in principle, a quantitative understanding of the fission fragment angular distribution associated with the chosen Surrogate reaction. Furthermore, we have concentrated here on a region of the nuclear chart for which it is empirically known that many of the relevant properties, such as transmission coefficients, vary only very slowly with mass number. Carrying out benchmark experiments, in which the Ratio approach is used to extract a known cross section, could help shed light on these issues.

The experiments required for a Ratio analysis are simpler than those that need to be carried out if a full Surrogate analysis (or a Surrogate analysis in the Weisskopf-Ewing limit) is planned. The primary advantage of considering relative branching ratios and relative cross sections lies in the fact that the number of direct-reaction events,  $N_\delta$ , does not need to be determined for a Ratio analysis. Furthermore, unlike in the full Surrogate treatment, it is not necessary to calculate the direct-reaction probabilities,  $F_\delta^{CN}(E, J, \pi)$ , or to model the decay of the compound nucleus.

The Ratio method is based on the Weisskopf-Ewing assumption and is therefore, in principle, only valid in this limit. We have seen that it is not *a priori* clear whether the Weisskopf-Ewing limit applies to a particular reaction in a given energy regime. This needs to be verified for each case of interest. At the same time, our calculations indicate that in situations where the Weisskopf-Ewing limit provides at least a rough approximation, the Ratio method can give useful results. It seems that small to moderate deviations from this assumption cancel in the Ratio approach. Thus, a Ratio analysis of a Surrogate experiment is a useful tool for obtaining a first estimate of an unknown cross section. Moreover, such an analysis can provide a valuable test for a result obtained from a complete Surrogate analysis.

The Ratio method is limited by the requirement that for obtaining an absolute result for an unknown cross section  $\sigma(a_1 + A_1 \rightarrow B_1^* \rightarrow c_1 + C_1)$  a reliable independent cross-section measurement for a similar reaction,  $a_2 + A_2 \rightarrow B_2^* \rightarrow c_2 + C_2$  must be available. Furthermore, it is required that a direct-reaction mechanism,  $D(d, b)B^*$ ,

and target-projectile combinations can be identified that make it possible to produce the compound nuclei,  $B_1^*$  and  $B_2^*$ , respectively.

One can expect reliable cross section estimates from the Ratio approach only when the two reactions that are analyzed,  $D_1(d, b)B_1^*$  and  $D_2(d, b)B_2^*$ , are sufficiently similar. When small systematic errors or small violations of the prerequisite assumptions, such as the validity of the Weisskopf-Ewing approximation or the absence of preequilibrium decays, affect both reactions in the same manner, it is likely that the effects cancel in part in the Ratio analysis. Uncorrelated errors and deviations, on the other hand, will increase the overall uncertainty in the final result. A reasonable definition of similarity might require that i) the same projectile initiates the compound-nucleus reactions that are compared, i.e.  $a_1 = a_2$ , and the same kind of decay (gamma emission, charged-particle emission, or fission) is considered in both cases; ii) the decays of the compound nuclei  $B_1^*$  and  $B_2^*$  have similar properties (number and kind of open channels, separation energies for the various channels, level densities in the residual nuclei, etc.); iii) the direct (Sur-

rogate) reactions which produce the compound nuclei employ the same mechanism,  $D(d, b)B^*$ , and projectile-ejectile combination,  $d - b$ , in both cases. All three conditions apply to the cases studied here.

### Acknowledgments

The authors appreciate inspiring discussions with L. A. Bernstein, H. C. Britt, J. Burke, C. Forssén, D. Gogny, A. Kerman, D. McNabb, J. B. Wilhelmy, and W. Younes on Surrogate reactions for fission studies. Careful readings of an early version of this manuscript by C. Forssén and W. Younes are gratefully acknowledged. This work was performed under the auspices of the U.S. Department of Energy by the University of California, Lawrence Livermore National Laboratory (LLNL) under contract No. W-7405-Eng-48. Partial funding was provided by the Laboratory Directed Research and Development Program at LLNL under project 04-ERD-057.

- 
- [1] W. Younes and H. C. Britt, Phys. Rev. C **67**, 024610 (2003).
  - [2] W. Younes and H. C. Britt, Phys. Rev. C **68**, 034610 (2003).
  - [3] J. Escher, L. Ahle, L. Bernstein, J. Church, F. S. Dietrich, C. Forssén, and R. Hoffman, Nucl. Phys. A **758**, 86c (2005).
  - [4] C. Forssén, L. Ahle, L. Bernstein, J. Church, F. Dietrich, J. Escher, and R. Hoffman, Nucl. Phys. A **758**, 130c (2005).
  - [5] J. Church et al., Nucl. Phys. A **758**, 126c (2005).
  - [6] J. Escher et al., in *Proceedings of the 21st Winter Workshop on Nuclear Dynamics*, edited by W. Bauer, R. Bellwied, and S. Panitkin, Breckenridge, Colorado, February 5–12, 2005 (EP Systema, Budapest, Hungary, 2005), pp. 49–56.
  - [7] C. Forssén et al., manuscript in preparation (2006).
  - [8] J. D. Cramer and H. C. Britt, Phys. Rev. C **2**, 2350 (1970).
  - [9] J. D. Cramer and H. C. Britt, Nucl. Sci. and Eng. **41**, 177 (1970).
  - [10] B. B. Back et al., Phys. Rev. C **9**, 1924 (1974).
  - [11] B. B. Back et al., Phys. Rev. C **10**, 1948 (1974).
  - [12] H. C. Britt and J. B. Wilhelmy, Nucl. Sci. and Eng. **72**, 222 (1979).
  - [13] M. Petit, M. Aiche, G. Barreau, et al., Nucl. Phys. A **735**, 347 (2004).
  - [14] C. Plettner et al., Phys. Rev. C **71**, 051602(R) (2005).
  - [15] J. Burke, L. Bernstein, J. Escher, et al., Phys. Rev. C **73**, 054604 (2006).
  - [16] P. Fröbrich and R. Lipperheide, *Theory of Nuclear Reactions* (Clarendon Press, Oxford, 1996).
  - [17] E. Gadioli and P. E. Hodgson, *Pre-Equilibrium Nuclear Reactions* (Clarendon Press, Oxford, 1992).
  - [18] F. S. Dietrich, Tech. Rep. UCRL-TR-201718, Lawrence Livermore National Laboratory, Livermore, CA (2004).
  - [19] W. Younes, H. C. Britt, J. A. Becker, and J. B. Wilhelmy, Tech. Rep. UCRL-ID-154194, Lawrence Livermore National Laboratory, Livermore, CA (2003).
  - [20] L. A. Bernstein, J. Burke, L. Ahle, J. A. Church, J. Escher, et al., Tech. Rep., Lawrence Livermore National Laboratory, Livermore, CA (2006).
  - [21] M. Uhl and B. Strohmaier, Tech. Rep. IRK 76/01, rev. 1978, Institut für Radiumforschung und Kernphysik, Vienna, Austria (1976).
  - [22] B. Strohmaier and M. Uhl, in *Nuclear Theory for Applications*, International Centre for Theoretical Physics (ICTP, Trieste, Italy, 1980), IAEA-SMR-43, p. 313.
  - [23] J. E. Escher and F. S. Dietrich, Tech. Rep. UCRL-TR-212509-Draft, Lawrence Livermore National Laboratory, Livermore, CA (2005).
  - [24] W. E. Ormand, private communication.
  - [25] T. Belgya, O. Bersillon, R. Capote, T. Fukahori, G. Zhi-gang, S. Goriely, M. Herman, A. V. Ignatyuk, S. Kailas, A. Koning, et al., *Handbook for calculations of nuclear reaction data: Reference input parameter library*, <http://www.nds.iaea.org/RIPL-2> (2005).
  - [26] A. Gilbert and A. G. W. Cameron, Can. J. Phys. **43**, 1446 (1965).
  - [27] S. Bjornholm and J. E. Lynn, Rev. Mod. Phys. **52**, 725 (1980).
  - [28] D. M. Brink, *Ph.D. thesis*, Oxford University (1955).
  - [29] P. Axel, Phys. Rev. **126**, 671 (1962).
  - [30] R. J. Howerton, R. E. Dye, P. C. Giles, J. R. Kimlinger, S. T. Perkins, and E. F. Plechaty, Tech. Rep. UCRL-50400, Lawrence Livermore National Laboratory, Livermore, CA (1983).
  - [31] Cross Section Evaluation Working Group, edited by P. Oblozinsky and M. Herman, *ENDF/B-VII beta2 Summary Documentation* (National Nuclear Data Center,

- Brookhaven National Laboratory, Upton, NY, 2006).
- [32] S. Gales, C. Stoyanov, and A. I. Vdovin, *Phys. Rep.* **166**, 125 (1988).
  - [33] S. Fortier et al., *Phys. Rev. C* **41**, 2689 (1990).
  - [34] S. Fortier et al., *Phys. Rev. C* **52**, 2401 (1995).
  - [35] A. Bonaccorso, *Phys. Rev. C* **51**, 822 (1995).
  - [36] B. L. Andersen, B. B. Back, and J. M. Bang, *Nucl. Phys. A* **147**, 33 (1970).
  - [37] B. D. Wilkins, J. P. Unik, and J. R. Huizenga, *Phys. Lett.* **12**, 243 (1964).
  - [38] H. C. Britt, W. R. Gibbs, J. J. Griffin, and R. H. Stokes, *Phys. Rev.* **139**, B354 (1965).
  - [39] H. C. Britt and F. Plasil, *Phys. Rev.* **144**, 1046 (1966).
  - [40] R. Vandenbosch, K. L. Wolf, J. Unik, C. Stephan, and J. R. Huizenga, *Phys. Rev. Lett.* **19**, 1138 (1967).
  - [41] K. L. Wolf, R. Vandenbosch, and W. D. Loveland, *Phys. Rev.* **170**, 1059 (1968).
  - [42] H. C. Britt, F. A. Rickey, and W. S. Hall, *Phys. Rev.* **175**, 1525 (1968).
  - [43] H. C. Britt and J. D. Cramer, *Phys. Rev.* **181**, 1634 (1969).
  - [44] V. M. Maslov, *Phys. Rev. C* **72**, 44607 (2005).